Monthly Notices of the ROYAL ASTRONOMICAL SOCIETY

MNRAS **545,** 1–7 (2026) https://doi.org/10.1093/mnras/staf2017
Advance Access publication 2025 November 14

Radially trapped overstable convective modes within a polytropic solar interior

Rekha Jain ★

School of Mathematical and Physical Sciences, University of Sheffield, Sheffield S3 7RH, UK

Accepted 2025 November 10. Received 2025 October 14; in original form 2025 August 22

ABSTRACT

We study overstable and unstable gravito-inertial waves in a weakly unstable polytropic atmosphere representing solar convection zone. We consider wave modes propagating at a small angle to the zonal direction near the equatorial region of the Sun. We find that the coriolis force plays an important role in stabilizing low radial order, long wavelength convective modes which otherwise would be unstable in the absence of rotation. Focusing solely on naturally trapped waves in the radial direction, we also compare the properties of these low frequency gravito-inertial wave modes with corresponding wave modes in a neutrally stable polytropic atmosphere in different sized finite domain. We find that the eigenfrequencies of gravito-inertial wave modes in a weakly unstable polytropic atmosphere are lower than those in a neutrally stable atmosphere, and that their propagation is confined to a narrower wavenumber range. These eigenfrequencies and the range of wavenumbers increase slightly as the angle of propagation increase.

Key words: Sun: interior – Sun: oscillations – Sun: rotation – stars: low-mass.

1 INTRODUCTION

Convection zone in the Sun drives turbulence affected by gravitational stratification, rotation and magnetic field. Prograde propagating vorticity waves are recurring features in theories of rotating solar convection zone at convective onset. Many linear studies have attributed them to compressional β-effect as well as conservation of law of potential vorticity in a stratified atmosphere (see G. A. Glatzmaier & P. A. Gilman 1981; Y. Bekki, R. H. Cameron & L. Gizon 2022b; B. W. Hindman & R. Jain 2022; R. Jain & B. W. Hindman 2023; R. Jain, B. W. Hindman & Blume. C. C. 2024). Simulation studies of non-linear rotating convection zone in spherical bodies with various assumptions have also been carried out (see for example, Y. Bekki, R. H. Cameron & L. Gizon 2022a, b; S. A. Triana et al. 2022, J. Bhattacharya & S. M. Hanasoge 2023; C. C. Blume, B. W. Hindman & L. I. Matilsky 2024). However, we have yet to fully grasp the effects of gravitational stratification, rotation and magnetic field on the low-frequency inertial waves that are driven by coriolis force in the Sun's interior. The challenge has further intensified with recent detection of equatorial Rossby waves (B. Löptien et al. 2018), critical and high-latitude inertial modes (L. Gizon et al. 2021) and high frequency retrograde modes (C. S. Hanson, S. M. Hanasoge & K. R. Sreenivasan 2022).

Helioseismology has revealed that the distribution of Buoyancy frequency, N in the Sun's interior is far from uniform (see for example, J. Christensen-Dalsgaard 2002). The lower region of the convection zone shows different distribution of N from its upper region and from the radiative zone below it. According to the standard solar model S, the square of the buoyancy frequency $N^2 < 0$ in the Sun's convection zone and therefore in general, the Sun's convection zone is globally unstable to convection. Noticing a layer in the solar convection zone where $|\frac{N^2}{\Omega^2}| << 1$ where Ω^2 is the square of the rotation rate, B. W. Hindman & R. Jain (2023) showed that the long wavelength (azimuthal order, $m \leq 30$) gravito-inertial waves propagating in the zonal direction are stabilized by the rotation in such a layer. It was shown explicitly by B. W. Hindman & R. Jain (2023) that the stability criterion for the prograde propagating gravito-inertial waves in the solar convection zone near the equator also depends on the acoustic cut-off frequency. In particular,

$$N^2 > -\frac{\Omega^2}{(k^2 + k_c^2)\mathcal{H}^2} \tag{1}$$

where k is the total wavenumber; $\mathcal{H}$ is a length scale that is related to the density scale height H and buoyancy frequency N i.e.

$$\frac{1}{\mathcal{H}} = \frac{1}{H} - \frac{2N^2}{g}. \tag{2}$$

Here, g is the constant gravitational acceleration and

$$k_c^2 = \frac{1}{4H^2}\left(1 - 2\frac{\mathrm{d}H}{\mathrm{d}r}\right). \tag{3}$$

The above criterion (1) suggests that stable waves can exist for weakly unstable stratification if $|N|$ is comparable to the rotation rate, Ω. Encouraged by this, B. W. Hindman & R. Jain (2023) investigated the stability of radially trapped waves propagating in the zonal direction in a weakly unstably stratified atmosphere and found the waves with small wavenumbers to be stable in such an atmosphere, due to rotation.

★ E-mail: R.Jain@sheffield.ac.uk

It is thus, believed that strong density stratification has influence in the Sun's convection zone and it is important to consider its effect without the assumption of Boussinesq fluid. In this paper, we will consider density stratification without Boussinesq approximation and examine waves in a neutrally stable as well as weakly unstably stratified polytropic atmosphere.

Gravito-inertial waves are likely to also propagate at an angle to the zonal direction. The numerical simulations of rotating spherical shells by B. W. Hindman, N. A. Featherstone & K. Julien (2020) clearly indicate the presence of Taylor columns and vorticity waves at the onset of the convection. These prograde propagating waves persist even when the flow becomes turbulent and although the columns are confined to the equatorial band, the waves are not always aligned to the zonal direction. At times, they are slightly inclined to the zonal direction with small latitudinal component.

Recently, R. Jain & B. W. Hindman (2023) investigated the latitudinal propagation of wave modes in a neutrally stable atmosphere and found that the low radial order wave modes are naturally trapped in radial direction for some inclination angles in a semi-infinite domain. Here, we want to explore the properties of such radially trapped wave modes, at a small angle to the zonal direction, in a weakly unstable polytropic atmosphere. Thus, in this paper, we focus on low-frequency gravito-inertial waves that propagate at a small angle to the zonal direction and compare their properties with the purely zonal wave-modes.

The properties of gravito-inertial waves in this study, will be influenced by rotation and gravitational stratification. The low-frequency gravito-inertial waves have been studied in various contexts and are referred to with different names in different literature. For example, in Geophysics, they are called as Thermal Rossby waves whereas in Astrophysics, these waves are generally referred to as overstable convective modes. The waves require either a curvature in the boundaries to have topological β-effect (see P. H. Roberts 1968; F. H. Busse 1970) or density stratification in the radial direction to produce compressional β-effect in fluid columns or vortices (see R. Hide 1966; G. A. Glatzmaier & P. A. Gilman 1981; B. W. Hindman & R. Jain 2022). In this paper, we consider plane parallel geometry and compressional β-effect due to stratification.

The paper is organized as follows. In Section 2, we describe our generic model and the assumptions. The governing equations derived for a polytropic atmosphere from this model are in Section 3. These equations are valid irrespective of whether the polytropic stratification is stable, unstable, or neutrally stable. We, first, examine the potentially complex eigenfrequencies that apply for globally unstable stratification in the limit of slow rotation. This is in the subsection *Semi-infinite domain*. Secondly, we compare the wave properties between neutrally stable and a weakly unstable polytrope for radially trapped waves in the subsection *Finite domain*. Finally, the brief conclusions are reported in Section 4.

2 THE MODEL

We investigate radial and latitudinal propagation of gravito-inertial wave modes near the equatorial region of the Sun. We thus, neglect the curvature of the Sun and consider a local plane-parallel Cartesian coordinate system whose origin is at the outer surface of the Sun's equator. We assume a constant gravity in the radial direction ($z = 0$ is the surface) i.e. $\mathbf{g} = -g\hat{\boldsymbol{z}}$ with $\hat{\boldsymbol{z}}$ pointing in the radial direction. The longitudinal and latitudinal directions point in the $\hat{\boldsymbol{x}}$ and $\hat{\boldsymbol{y}}$ directions, respectively. The rotation vector is $\Omega = \Omega\hat{\boldsymbol{y}}$. As was shown by R. Jain & B. W. Hindman (2023), the propagation of small amplitude planar waves in such a model is governed by

$$\frac{\mathrm{d}^2\Psi}{\mathrm{d}z^2} + k_z^2(z)\,\Psi = 0, \tag{4}$$

where

$$k_z^2(z) = \frac{\omega^2 - (\omega_{\rm ac}^2 + 4\Omega^2)}{c_{\rm s}^2} - k_h^2\left(1 - \frac{N^2}{\omega^2}\right) + \frac{2\Omega k_x}{\omega\mathcal{H}} + \frac{4k_y^2\Omega^2}{\omega^2} \tag{5}$$

is a function of depth. In equation (4), Ψ is a scaled Lagrangian pressure fluctuation δP of the wave, i.e

$$\delta P(x, y, z, t) = \rho_0^{1/2}\Psi(z)e^{i(k_x x + k_y y - \omega t)}. \tag{6}$$

Here, ω is the temporal frequency and $k_h^2 = k_x^2 + k_y^2$ with $k_x(= k_h\cos\chi)$ and $k_y(= k_h\sin\chi)$ as the wavenumbers in the x and y directions, respectively. The parameter χ denotes the angle between the propagation wave vector and the x-axis (also referred to as zonal or longitudinal direction). We only consider positive longitudinal wavenumbers, $k_x > 0$ and so the waves propagate in the prograde direction if the frequency is positive, $\omega > 0$, and in the retrograde direction for negative frequencies, $\omega < 0$. Thus $\chi = 0$ indicates the direction of horizontal (zonal) propagation, with positive phase speed, corresponding to pure prograde propagation and $\chi = \pi/2$ indicates pure northward propagation. The notation ρ_0 in equation (6) is the background density.

It is apparent from equation (5) that the vertical wavenumber k_z is depth (radially) dependent. The square of the buoyancy frequency, N^2, is defined as follows

$$N^2(z) = g\left(\frac{1}{H} - \frac{g}{c_{\rm s}^2}\right); \qquad H^{-1} = \left(\frac{1}{\rho_0}\frac{\mathrm{d}\rho_0}{\mathrm{d}z}\right), \tag{7}$$

where H is the density scale height and c_s^2 is the square of the sound speed. The scale height $\mathcal{H}$ in the third term in equation (5) is also related to H and N^2 as shown in equation (2).

The square of the acoustic cut-off frequency, ω_{ac} in equation (5) is defined as

$$\omega_{\rm ac}^2 \equiv \frac{c_{\rm s}^2}{4H^2}\left(1 - 2\frac{\mathrm{d}H}{\mathrm{d}z}\right). \tag{8}$$

We can obtain the wave cavity for trapped modes by considering $k_z^2 = 0$ from equation (4). Note that equation (5) is a fourth order polynomial equation in ω and hence there are four solutions. Two of the solutions correspond to high-frequency acoustic waves and the other two are low-frequency gravito-inertial waves.

Since we are interested in the low frequency gravito-inertial waves, we consider the **low-frequency limit**, $\frac{\omega}{2\Omega} << 1$, of equation (5), and ignore $\frac{\omega^2 - 4\Omega^2}{c_{\rm s}^2}$ term to yield

$$k_z^2 = -\frac{\omega_{\rm ac}^2}{c_{\rm s}^2} + \frac{2\Omega k_x}{\omega\mathcal{H}} - k_h^2\left(1 - \frac{N^2}{\omega^2}\right) + \frac{4k_y^2\Omega^2}{\omega^2}. \tag{9}$$

Note that the density scale height H decreases with radius in the Sun. Therefore, $\frac{\omega_{ac}^2}{c_{\rm s}^2} > 0$ from equation (8). This suggests from equation (9) that the wave cavity can exist if

$$k_z^2 = \left[\frac{2\Omega k_x}{\omega\mathcal{H}} + k_h^2\frac{N^2}{\omega^2} + \frac{4k_y^2\Omega^2}{\omega^2}\right] - \left(k_h^2 + \frac{\omega_{ac}^2}{c_s^2}\right), \tag{10}$$

is positive, i.e. the terms inside the square bracket exceeds the terms in the round brackets. As was pointed out by B. W. Hindman & R. Jain (2022), the first term, $\frac{2\Omega k_x}{\omega\mathcal{H}}$, is due to the coriolis term and is large for low frequencies i.e. $\frac{\omega}{\Omega} < 1$. This term is responsible for gravito-inertial wave cavities in radial direction. Also, the direction of waves depends on the wave speed ω/k_x. The second term in the

square bracket is a buoyancy term and is responsible for internal gravity wave cavity, provided $N^2 > 0$. Both retrograde and prograde waves are possible. Even for $k_x \to 0$, we can have internal gravity wave cavity if the buoyancy term dominates or inertial waves in the absence of stratification. If all three terms in the square bracket are large, we can have a cavity for the gravito-inertial waves. Even in the solar convection zone where $N^2 \leq 0$, the coriolis term and the last term inside the square bracket can be large for large k_x and for rapid rotation respectively.

For $\frac{|N|}{\Omega} >> 2$, equation (10) yields

$$\frac{\omega}{\Omega} \approx \frac{k_x}{K^2\mathcal{H}}\left[1 \pm \left(1 + \frac{k_h^2}{k_x^2}\frac{N^2}{\Omega^2}K^2\mathcal{H}^2\right)^{1/2}\right]. \tag{11}$$

where $K^2 = \frac{\omega_{ac}^2}{c_s^2} + k_z^2 + k_h^2$.

These are internal-gravity waves that propagate in prograde or retrograde direction. Clearly, the prograde waves propagate faster compared to the retrograde waves for $k_x \neq 0$. For $k_x = 0$, both waves have the same magnitude, and we have northward and southward propagating waves with the same speed.

On the other hand, for *rapid rotation* such that $\frac{k_h}{k_y}\frac{|N|}{\Omega} << 1$, we once again obtain two solutions:

$$\frac{\omega}{\Omega} \approx \frac{k_x}{K^2\mathcal{H}} \pm \left(\frac{k_x^2}{K^4\mathcal{H}^2} + 4\frac{k_y^2}{K^2}\right)^{1/2}. \tag{12}$$

Prograde wave is faster than Retrograde for $k_x \neq 0$ and $k_y \neq 0$. Prograde propagating waves are also sometimes referred to as thermal Rossby waves.

For $k_y = 0$, we only have prograde propagating waves,

$$\left(\frac{\omega}{\Omega}\right)_+ \approx \frac{2k_x}{K^2\mathcal{H}}, \tag{13}$$

which are studied in detail, in B. W. Hindman & R. Jain (2022). The second term inside the parenthesis in equation (12) is the modification to thermal Rossby waves due to non-zero k_y. For $k_x = 0$, $\left(\frac{\omega}{\Omega}\right)_\pm \approx \pm 2\frac{k_y}{K}$ from equation (12), resulting in Northward and Southward propagating waves with same magnitude but primarily an inertial oscillation.

The competing effects of coriolis force, buoyancy and the angle of propagation leads to either gravito-inertial waves or internal gravity waves or acoustic waves. In the next section, we focus on the properties of low frequency gravito-inertial waves in a polytropic atmosphere relevant to low-mass stars such as the Sun.

3 POLYTROPIC ATMOSPHERE

We consider a polytropic atmosphere in the domain $z \in (-\infty, 0]$ such that all thermodynamic parameters are power-law functions of the height coordinate, z. Equation (4) can thus be transformed into Whittaker's Equation (see for details, R. Jain & B. W. Hindman (2023))

$$\frac{\mathrm{d}^2\Psi}{\mathrm{d}\xi^2} + \left[\frac{\kappa}{\xi} - \frac{1}{4} - \frac{\nu(\nu-1)}{\xi^2}\right]\Psi = 0, \tag{14}$$

where

$$\xi = -2k_h\sqrt{1-\varpi^2}\,z \tag{15}$$

is a non-dimensional depth and

$$\kappa = \frac{1}{\sqrt{1-\varpi^2}}\left[\left(\frac{\alpha+1}{2\gamma}\right)\frac{\omega^2 - 4\Omega^2}{gk_h} + \frac{(\alpha-\hat{\alpha})}{2\gamma\hat{\alpha}}\left(\frac{gk_h}{\omega^2}\right) + \left(\alpha - \frac{2(\alpha-\hat{\alpha})}{\gamma\hat{\alpha}}\right)\left(\frac{\Omega}{\omega}\right)\frac{k_x}{k_h}\right]. \tag{16}$$

The parameter $\nu\left(=\frac{\alpha+2}{2}\right)$ depends on stratification through the polytropic index α. For an adiabatic exponent γ, a neutrally stable atmosphere is $\hat{\alpha} \equiv (\gamma-1)^{-1}$. Thus, a polytropic atmosphere is neutrally (un)stable to convective overturning if $\alpha(<) > \hat{\alpha}$.

The parameter ϖ^2 used in equations (15) and (16) is defined as

$$\varpi^2 \equiv \frac{k_y^2}{k_h^2}\frac{4\Omega^2}{\omega^2} = \frac{4\Omega^2}{\omega^2}\sin^2\chi, \tag{17}$$

and governs the nature of the low frequency gravito-inertial waves in a polytropic atmosphere. For $\varpi^2 < 1$, we have radially trapped modes where as $\varpi^2 > 1$ gives rise to continuous spectrum of retrograde propagating waves into solar interior. Note that the radial eigenvalue κ can be obtained by applying appropriate boundary conditions.

The general solution of equation (14) is given by the sum of Kummer's Confluent hypergeometric functions of the first and second kind, namely M and U functions. In the following subsections, we will investigate the solution separately in a semi-infinite domain $z \in (-\infty, 0]$ and a finite domain $z \in [-D, 0]$ with D denoting the depth of the convection zone from the surface $z = 0$. For appropriate boundary conditions in the radial direction, Whittaker's Equation generates a discrete spectrum of eigenmodes, with κ as the eigenvalue. Since κ is a function of the frequency, each eigenmode will possess a specific eigenfrequency, ω_n with n as the radial order of the mode and $\kappa_n = \kappa_n(k_h)$ the nth eigenvalue.

In a non-dimensional form, the local dispersion relation (16) can be written as

$$\left[1 - \frac{4\sin^2\chi}{\tilde{\omega}^2}\right]^{1/2}\kappa = A\left(\tilde{\omega}^2 - 4\right)\frac{\epsilon}{m} + \frac{mS}{\tilde{\omega}^2} + \left[\frac{(\alpha - 4S\epsilon)}{\tilde{\omega}}\right]\cos\chi, \tag{18}$$

where

$$\tilde{\omega} = \frac{\omega}{\Omega}, \quad m = k_h R, \quad \epsilon = \frac{\Omega^2 R}{g}, \quad S = \frac{(\alpha-\hat{\alpha})}{2\gamma\hat{\alpha}\epsilon}, \quad A = \frac{\alpha+1}{2\gamma}.$$

For a regular solution in the semi-infinite domain $(-\infty, 0]$, the eigenvalue κ takes on discrete values that depend on the radial order n and the polytropic index α, i.e.

$$\kappa_n = n + 1 + \frac{\alpha}{2}, \tag{19}$$

and the eigenfunction (see equations 6) is given by

$$\delta P(z, x, y, t) = \mathcal{C}_n z^{\alpha+1} e^{k_h\sqrt{1-\varpi^2}z}\mathcal{L}_n^{(\alpha+1)}\left(-2\sqrt{1-\varpi^2}k_h z\right) e^{i\left(k_x x + k_y y - \omega t\right)}. \tag{20}$$

Here $\mathcal{C}_n$ is an arbitrary constant and $\mathcal{L}_n^{\alpha+1}$ is the nth-order Associated Laguerre Polynomial. For radially trapped waves, we require $\varpi^2 < 1$ (see also R. Jain & B. W. Hindman 2023). In what follows, we will consider such radially trapped waves in detail. In particular, we want to investigate if the modes that are unstable in the absence of rotation, could be stabilized in the presence of coriolis force. If so, for what wavelengths?

3.1 Semi-infinite domain: slow rotation

In this subsection, we investigate eigenfrequencies of the radially trapped gravito-inertial waves in a slowly rotating atmosphere in the domain $(-\infty, 0]$. For slowly rotating atmosphere, ϵ is very small. Thus, we expand $\frac{\omega_n}{\Omega_n}$ in powers of ϵ. Ignoring $O(\epsilon^2)$,

$$\frac{\omega_n}{\Omega_n} \approx a_0 + a_1\epsilon. \tag{21}$$

We investigate only the radially trapped modes in this section i.e. $\left|\frac{\omega_n}{\Omega_n}\right|^2 >> 4\sin^2\chi$. In this limit

$$\left[1 - \frac{4\sin^2\chi}{\left|\frac{\omega_n}{\Omega_n}\right|^2}\right]^{1/2} \approx 1 - \frac{2\sin^2\chi}{\left|\frac{\omega_n}{\Omega_n}\right|^2}, \tag{22}$$

which yields, using equation (18)

$$a_0 = \frac{\alpha\cos\chi \pm \left[\alpha^2\cos^2\chi + 4\kappa_n(2\kappa_n\sin^2\chi + mS)\right]^{1/2}}{2\kappa_n}, \tag{23}$$

and

$$a_1 = \frac{4a_0 S\cos\chi - \frac{A}{m}a_0^2(a_0^2 - 4)}{(\alpha\cos\chi - 2a_0\kappa_n)}.$$

In the above equations, κ_n is the nth eigenvalue and ω_n is the frequency of nth radial order mode. The' $+$ $(-)$' sign in equation (23) yield fast(slow) gravito-inertial trapped waves in a slowly rotating, polytropically stratified atmosphere. For a weakly unstable polytropic atmosphere $S < 0$. Thus, depending on the discriminant in equation (23), we can obtain complex eigenfrequencies. From equations (21) and (23), we have

$$\omega_n = \frac{\alpha\Omega\cos\chi}{2\kappa_n} \pm \left[\frac{\alpha^2\Omega^2\cos^2\chi}{4\kappa_n^2} + \frac{\left(\frac{gk_h(\alpha-\hat{\alpha})}{2\gamma\hat{\alpha}\Omega^2} + 2\sin^2\chi\kappa_n\right)\Omega^2}{\kappa_n}\right]^{1/2}. \tag{24}$$

Despite the atmosphere being neutrally unstably stratified ($\hat{\alpha} > \alpha$), a mode can be stabilized by rotation if the mode has sufficiently low k_hR and low radial order n. The mode is unstable for a threshold spherical harmonic degree, k_hR that exceeds

$$k_hR > -\frac{\left(\alpha^2\cos^2\chi + 8\sin^2\chi\kappa_n^2\right)}{4\kappa_n S}. \tag{25}$$

This threshold k_hR increases as the unstably stratified atmosphere becomes stronger (i.e. $|S|$ becomes smaller). Also note that the threshold k_hR increases with increasing χ. Thus, a mode propagating at an angle to the zonal direction has increased threshold k_hR compared to a mode with same radial order propagating purely in the zonal direction. We now examine how stability of the mode varies with different χ for a given S.

We consider a weakly unstable atmosphere with $S = -5\times10^{-3}$ and investigate the stability of the $n = 0$ modes propagating at different angles χ to the zonal axis. Fig. 1 shows real (left panel) and imaginary (right panel) parts of $\frac{\omega_n}{\Omega_n}$ as a function of k_hR for such $n = 0$ modes. The real and imaginary part of eigenfrequencies are obtained from equations (23) and (24) for $n = 0$. Various coloured curves are for different values of χ. On the left panel, the filled circle (dashed) curves are for fast (slow) modes. Only the points that satisfy $2\sin\chi < \left|\frac{\omega_n}{\Omega_n}\right| < 1$ are shown in both panels. As the angle of propagation increases, the real part of eigenfrequencies increase for a given k_hR. Also, the threshold k_hR beyond which we have the complex conjugate pair increases with χ. The fast and slow modes correspond to overstable convective modes when they have purely real frequencies. Such modes have been convectively unstable and

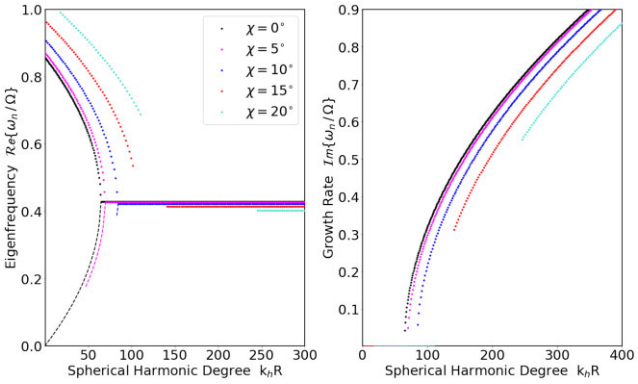

Figure 1. Complex eigenfrequencies of fast (filled circles) and slow (dashed) radially trapped gravito-inertial modes as a function of Spherical Harmonic Degree, k_hR in a semi-infinite domain. All curves are for $n = 0$ mode. Different colours are for different angles of propagation $\chi = 0°, 5°, 10°, 15°$, and $20°$. The assumption of radially trapped mode in a slow rotating atmosphere (see equations (23) and (24)) allows only certain eigenfrequencies. Low to moderate wavenumbers show overstable convective modes with purely real eigenfrequencies whereas for the higher wavenumbers, we have unstable wave modes.

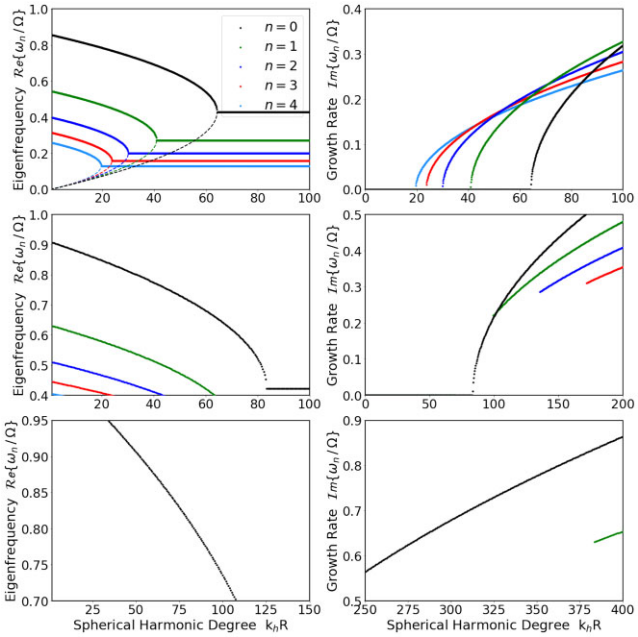

Figure 2. Complex eigenfrequencies of fast (filled circles) and slow (dashed) radially trapped gravito-inertial modes as a function of Spherical Harmonic Degree, k_hR in a semi-infinite domain. Only first five radial order modes are shown with different colour and for different angles of propagation $\chi = 0°$ (top), $10°$ (middle) and $20°$ (bottom). The assumption of slow rotation allows only certain eigenfrequencies. Low to moderate wavenumbers show overstable convective modes with purely real eigenfrequencies whereas for the higher wavenumbers, we have unstable wave modes.

without any oscillatory part in the absence of rotation. When the two solutions are complex, we have unstable, oscillatory convective modes that have same speed and they propagate in the prograde direction. All modes are overstable for low-to-moderate k_hR.

Now we consider other radial order modes for different χ for the same value of S. Fig. 2 displays the real (left column) and imaginary part (right column) of the complex eigenfrequencies for

low-frequency radially trapped gravito-inertial waves in the limit of slow rotation. For clarity, we only show the first five radial orders ($n = 0, 1, 2, 3, 4$) and denote them with different colors black, green, blue, red and light-blue.

The top row in Fig. 2 is for $\chi = 0^\circ$. The left-hand panel shows two types of gravito-inertial waves: fast waves with thick filled circles and slow waves with dashes. Once again, both types of waves are prograde propagating and their real frequencies merge at some wavenumber. As mentioned, at this threshold wavenumber and beyond, the two waves have conjugate pair with the same real frequencies and oppositely signed imaginary parts. It is clear that for low to moderate wavenumbers, both types of waves propagating in zonal direction are infact overstable convective modes. The right-hand panel illustrates the positive imaginary root i.e. the growth rate. The waves are unstable when they have complex eigenfrequencies. These unstable waves have a growth rate for moderate values of azimuthal order ($k_h R = k_x R$ for $\chi = 0^\circ$) as shown in the top right panel. This was also reported in B. W. Hindman & R. Jain (2023), where only the case of $\chi = 0^\circ$ was considered. Recall that the fast and slow gravito-inertial waves have been referred to as Thermal Rossby waves at and beyond the threshold in F. H. Busse (1986) i.e. the unstable and marginally stable modes collectively have been called as Thermal Rossby waves, whereas B. W. Hindman & R. Jain (2022) referred the entire solution (stable + unstable) as Thermal Rossby wave.

Since we are only focusing on the radially trapped waves in the limit of slow rotation, we only display the stable and unstable solutions for waves that satisfy $2\sin\chi \ll |\frac{\omega}{\Omega}| \ll 1$. These are shown in the middle row for $\chi = 10^\circ$ and in the bottom for $\chi = 20^\circ$. Only low-order, fast gravito-inertial waves are found to be radially trapped in this limit. Once again, for low to moderate spherical harmonic degrees $k_h R$, we have overstable convective modes (with purely real eigenfrequencies) and unstable modes for higher $k_h R$. However, the magnitude of the eigenfrequencies for $\chi \neq 0$ are higher compared to the waves that propagate in purely zonal direction ($\chi = 0^\circ$). The threshold $k_h R$ beyond which the wave modes are unstable is also large as expected from equation (25).

3.2 Finite domain

The solar convection zone is believed to be about 200 Mm in depth and as specified by model S (J. Christensen-Dalsgaard et al. 1996), the square of the buoyancy frequency, N^2, shows a sharp rise at the bottom of the convection zone (see fig. 1 in B. W. Hindman & R. Jain 2023). We consider the thin layer where this sudden change in N^2 occurs at the interface where the gravito-inertial waves undergo total reflection. We thus apply a reflective boundary condition at this interface, and adopt a condition of vanishing lagrangian pressure fluctuation at this interface, i.e. $\delta P(z = -D) = 0$. We will examine the effect of different depth of the interface on eigenfrequencies of waves and so we consider three different depths, $D = 100$ Mm, 200 Mm, and 300 Mm. Along with the regularity condition at the origin ($z = 0$), we now obtain the following dispersion relation:

$$M(-\eta, \alpha + 2, 2\sqrt{1 - \varpi^2} k_h D) = 0, \tag{26}$$

where $\eta = \kappa - \frac{\alpha}{2} + 1$ with κ is given by equation (16). We are interested in the eigenfrequencies of gravito inertial waves that propagate at an angle to the zonal direction in a finite domain with $N^2 < 0$ and also want to compare them with the corresponding gravito-inertial waves in a neutrally stable atmosphere i.e. $N^2 = 0$. For both these atmospheres, we consider wave frequencies that satisfy $2\sin\chi \leq \frac{\omega}{\Omega}$. This enables us to have a direct comparison

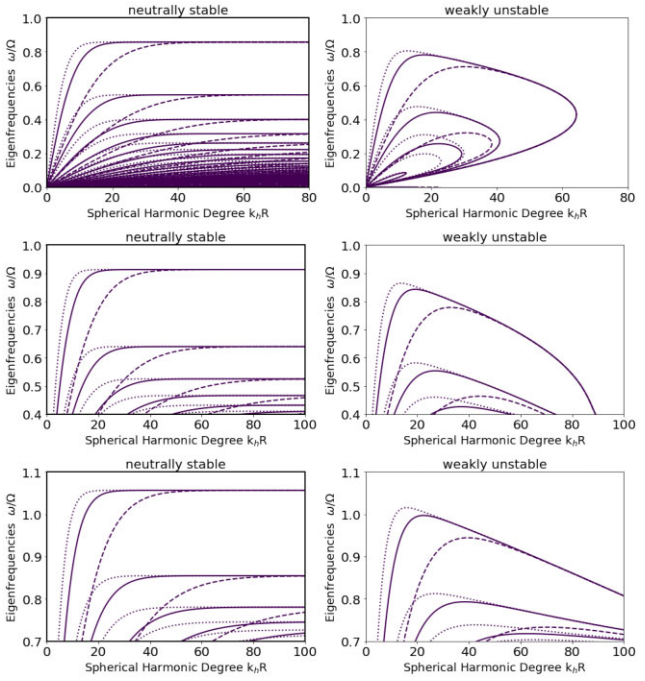

Figure 3. Eigenfrequencies, ω/Ω, for gravito-inertial modes as a function of Spherical Harmonic Degree, $k_h R$, for neutrally stable (left column) and weakly unstable (right column) polytropic atmosphere in a finite domain D. The radial orders $n = 0, 1, 2, 3, 4$, etc. are shown for each finite domain, D = 100 Mm (dashed), 200 Mm (solid), and 300 Mm (dotted). The top, middle and bottom rows are for various angles of propagation, $\chi = 0^\circ$, 10°, and 20°, respectively. In all figures, $2\sin\chi \leq |\frac{\omega}{\Omega}|$.

with the corresponding waves in a weakly unstably stratified semi-infinite region discussed in previous section (see also, R. Jain & B. W. Hindman 2023 for neutrally stable atmosphere). In Fig. 3, we plot eigenfrequencies as a function of spherical harmonic degree $k_h R$ for three different values for depths $D = 100$ Mm (dashed), 200 Mm (solid), and 300 Mm (dotted). The top, middle and bottom rows are for angle of propagation, $\chi = 0^\circ$, 10°, and 20°, respectively. The left column shows curves for a neutrally stable polytropic atmosphere ($N^2 = 0$) and the right column for a weakly unstable polytropic atmosphere. In all figures, the uppermost curve corresponds to modes that lack nodes in radius i.e. $n = 0$. The radially trapped modes with $n > 0$ also have positive frequencies with even higher radial order modes showing accumulation at zero frequencies for the neutrally stable atmosphere. On the other hand, the nature of gravito-inertial waves is very different in the weakly unstable atmosphere as shown in the right column. The corresponding waves have relatively lower eigenfrequencies and restricted range of $k_h R$.

As was also noted in the semi-infinite domain solutions (see the previous subsection), here also only low radial order trapped modes exist for $\chi = 0^\circ$ regardless of the type of stratification. The modes of very low $k_h R$ are not naturally trapped except when waves have purely zonal propagation i.e. for $\chi = 0^\circ$. However, both types of waves, slow and fast, are prograde propagating for $\chi = 0^\circ$ where as only fast modes exist for $\chi > 0^\circ$ with $2\sin\chi < \frac{\omega}{\Omega}$.

It is noticeable that as the depth increases, there are more higher radial order modes that satisfy $\frac{\omega}{\Omega} > 2|\sin\chi|$ as is shown in Fig. 3 (for example, compare the dotted curves with dashed). The eigenfrequencies are slightly higher for $D = 300$ Mm compared to $D = 100$ Mm and the modes with relatively low wavenumbers also exist.

3.3 g-modes coupling

As was mentioned in the earlier section, the distribution of N^2 with depth, shows a sudden increase in N^2 between the convection zone and the radiative interior (see fig. 1 in J. Christensen-Dalsgaard et al. 1996; see also B. W. Hindman & R. Jain 2023). Thus, at this interface, it is possible that coupling between g-modes and the gravito-inertial waves occur. In other words, the dispersion curves of prograde propagating g-modes that reside in the stable radiative zone beneath the interface, and the gravito-inertial modes that reside above the interface, are expected to cross at certain eigenfrequencies with avoided crossings at these eigenfrequencies.

With a view to investigate these avoided crossings further, we consider a two-layer model as was also studied in B. W. Hindman & R. Jain (2023) for $\chi = 0^\circ$. We attach a sheet of isothermal atmosphere, mimicking radiative zone, below the weakly unstable polytropic layer of finite depth D. The thickness L of the isothermal atmosphere is assumed to be 500 km. We keep the parameters D and S fixed as in previous sections $D = 200$ Mm and $S = -5 \times 10^{-3}$. The boundary conditions for this two layer model is $\delta P = 0$ (at $z = 0$) and $\frac{\mathrm{d}\delta P}{\mathrm{d}z} = 0$ (at $z = -(D + L)$). Across the interface, $z = -D$ we require δP and $\frac{\mathrm{d}\delta P}{\mathrm{d}z}$ to be continuous. Using these boundary conditions and the matching across $z = -D$, we obtain the following dispersion relation:

$$\frac{K_{\rm iso}\sin(K_{\rm iso}L) + \left[k_h\cos\chi - \left(\frac{\alpha+2}{2D}\right)\right]\cos(K_{\rm iso}L)}{\cos(K_{\rm iso}L)} - \frac{2k_h\sqrt{1-\varpi^2}M'\left(\nu-\kappa_n, 2\nu, 2k_h\sqrt{1-\varpi^2}D\right)}{M\left(\nu-\kappa_n, 2\nu, 2k_h\sqrt{1-\varpi^2}D\right)} = 0, \quad (27)$$

where the radial wavenumber, denoted by $K_{\rm iso}$, within the isothermal atmosphere now has all the terms constant with depth (see equation 5) i.e.

$$K_{\rm iso}^2 = \frac{\omega^2 - \omega_{\rm ac}^2 - 4\Omega^2}{c_{\rm s}^2} - k_h^2\left(1 - \frac{N^2}{\omega^2}\right) + \frac{2\Omega k_x}{\omega\mathcal{H}} + \frac{4k_y^2\Omega^2}{\omega^2}. \quad (28)$$

In equation (27), M' is the derivative of the M Kummer function with respect to z (refer to equation 15). We solve this dispersion relation for a set of fixed parameters to obtain eigenfrequencies ω_n/Ω_n for varying k_hR.

Fig. 4 displays the eigenfrequencies as a function of k_hR for prograde propagating g modes and the gravito-inertial modes of the finite domain. These are blue curves in the left column indicated by panels (a). The gravito-inertial modes that have been obtained by ignoring the g-mode cavity are also superimposed with black dotted curves (refer to subsection 3.2). The top, middle and bottom rows are for $\chi = 0^\circ$, 10° and 20°, respectively. As expected, an avoided crossing can be seen wherever the eigenfrequencies of the two types of modes cross each other. These avoided crossings are shown in the right column in panels (b) for each of the three angles of propagation, χ. The range of eigenfrequencies where the two types of modes, the g modes and the gravito-inertial modes, have resonance appears quite small. The eigenfrequencies and the spherical harmonic degree k_hR, where such avoided crossing occur increases with angle χ. Note that $k_hR = k_xR = m$ for $\chi = 0^\circ$ (see also, B. W. Hindman & R. Jain 2023).

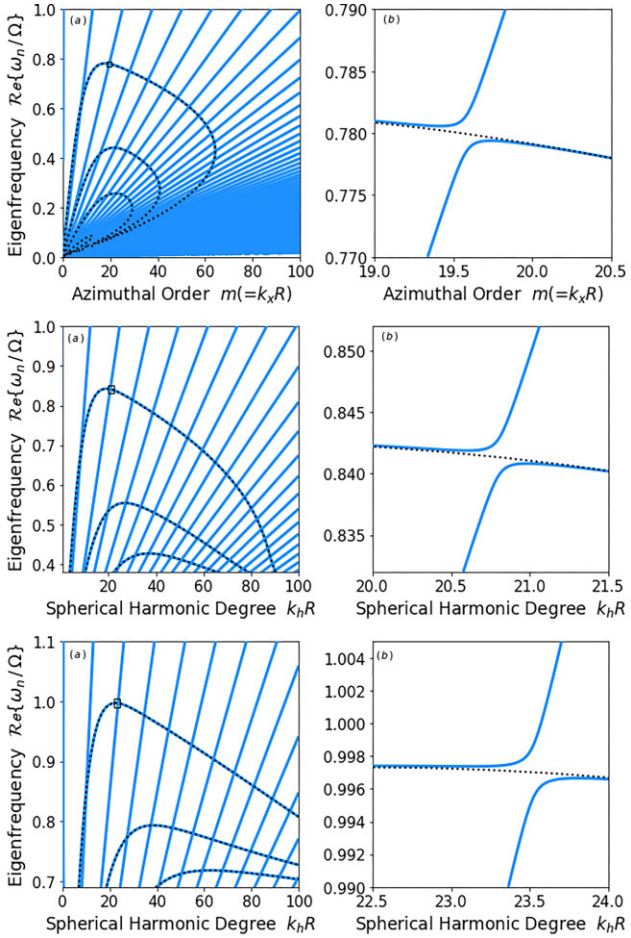

Figure 4. Real part of eigenfrequencies obtained from a two layer model consisting of a stably stratified radiative interior and a weakly unstable polytropically stratified convection zone layer. The blue diagonal streaks are the solutions of g-modes in the radiative interior and the blue with black dotted curves are solutions of gravito-inertial waves that were obtained in the previous section (refer Fig. 3) for the case when the bottom of the convection zone had perfectly reflecting boundary with $D = 200$ Mm. The top, middle and bottom rows are for $\chi = 0^\circ$, 10°, and 20°. The panel (b) in all three rows show zoom-in view of the avoided crossing that is marked by the small box in panel (a).

4 CONCLUSION

In this paper, we have investigated the low-frequency gravito-inertial waves propagating at a small angle, χ to the zonal direction in a compressible, polytropically stratified atmosphere representing the Sun's convection zone. Using an analytical model valid for a general polytropic index, we explored eigenfrequencies of radially trapped wave modes in a weakly unstable polytrope. We found that in the semi-infinite domain, both slow and fast wave modes are naturally trapped in the radial direction for $\chi = 0^\circ$ and they propagate in the prograde direction but only fast wave-modes persist for an angle of propagation $\chi = 0^\circ$. In order to compare with previous studies, we also examined the eigenfrequencies of the wave-modes in a finite domain for a neutrally stable and a weakly unstable polytropic atmosphere. In a neutrally stable atmosphere, for a zonal propagation (i.e. $\chi = 0^\circ$), the slow waves become degenerate with a zero frequency wave and only the fast wave perseveres as a prograde propagating wave and is naturally trapped in the radial direction (see also, B. W. Hindman & R. Jain 2022). However, when non-parallel propagation to the zonal direction is considered in a neutrally stable polytropic atmosphere, waves with both, prograde and retrograde propagation exist but only prograde propagating

waves are naturally trapped in the radial direction (see R. Jain & B. W. Hindman 2023).

B. W. Hindman & R. Jain (2023) studied the properties of the overstable and unstable wave modes that exist when the polytrope is weakly unstable to convective overturning. They considered purely zonal propagating wave modes, i.e. $\chi = 0^\circ$. They found that both, slow and fast wave modes of low radial orders and long wavelengths can be stabilized due to rotation. These were also naturally trapped waves in the radial direction. Here, we extended the study to explore the possibility of $\chi = 0^\circ$, in the limit of slow rotation and found that only fast wave modes of low radial orders exist such that $2\sin\chi < |\frac{\omega}{\Omega}| < 1$ and these are stabilized by rotation for moderate to long wavelengths. Note that these wavelengths are longer for $\chi = 0^\circ$ compared to for $\chi = 0^\circ$. As illustrated in Fig. 2, there exists a wavelength threshold of convergence (at marginal stability) and beyond, the fast and slow wave-modes become a complex conjugate pair (only the positive imaginary root is illustrated) for higher orders. When the fast and slow wave-modes have purely real frequencies, the modes correspond to overstable convective modes. In the absence of rotation, both the fast and slow waves would have been otherwise convectively unstable and non-oscillatory. When the mode frequencies are complex, the two solutions correspond to unstable, oscillatory convective modes that travel prograde at the same speed. These unstable modes have a growth rate comparable with their oscillation frequency for moderate values of the spherical harmonic degree $k_h R$ (for $\chi = 0^\circ$, $k_h R = k_x R = m$). For non-parallel propagation, only low radial-order fast modes that are naturally trapped in the radial direction were considered. These were found to be overstable convective modes for low to moderate wavenumbers $k_h R$ unlike for parallel propagation where both slow and fast gravito-inertial waves are overstable convective modes in a weakly unstable polytropic atmosphere. As was shown in equation (25), this threshold wavenumber increases for $\chi > 0^\circ$.

We also investigated the possibility of coupling of g-modes with prograde propagating gravito-inertial modes that reside in the lower region of the convection zone. The common frequencies of the two modes may be useful for studying the g-mode cavity if the gravito-inertial waves (Thermal Rossby waves) can be observed.

ACKNOWLEDGEMENTS

I thank Dr B. W. Hindman (University of Colorado, USA) for many useful discussions on this topic.

DATA AVAILABILITY

The data behind the figures can be obtained from the author.

REFERENCES

Bekki Y., Cameron R. H., Gizon L., 2022a, A&A, 662, A16
Bekki Y., Cameron R. H., Gizon L., 2022b, A&A, 666, A135
Bhattacharya J., Hanasoge S. M., 2023, ApJS, 264, 21
Blume C. C., Hindman B. W., Matilsky L. I., 2024, ApJ, 966, 18
Busse F. H., 1970, J. Fluid Mech., 44, 441
Busse F. H., 1986, J. Fluid Mech., 173, 545
Christensen-Dalsgaard J., 2002, Rev. Mod. Phys., 74, 1073
Christensen-Dalsgaard J., Dappen W., Ajukov S. V., Anderson E. R., Antia H. M., Basu S., Baturin V. A., Berthomieu G., 1996, Science, 272, 1286
Gizon L. et al., 2021, A&A, 652, L6
Glatzmaier G. A., Gilman P. A., 1981, ApJS, 47, 103
Hanson C. S., Hanasoge S. M., Sreenivasan K. R., 2022, Nat. Astron., 6, 708
Hide R., 1966, Philos. T. Roy. Soc. Lond., 259, 615
Hindman B. W., Jain R., 2022, ApJ, 932, 68
Hindman B. W., Jain R., 2023, ApJ, 943, 127
Hindman B. W., Featherstone N. A., Julien K., 2020, ApJ, 898, 120
Jain R., Hindman B. W., 2023, ApJ, 958, 48
Jain R., Hindman B. W., C. B., 2024, ApJ, 965, 48
Löptien B., Gizon L., Birch A. C., Schou J., Proxauf B., Duvall T. L., Bogart R. S., Christensen U. R., 2018, Nat. Astron., 2, 568
Roberts P. H., 1968, Philos. T. Roy. Soc. Lond. Series A, 263, 93
Triana S. A., Guerrero G., Barik A., Rekier J., 2022, ApJ, 934, L4

This paper has been typeset from a TEX/LATEX file prepared by the author.